

Three-dimensional Simulations of Current Density Distributions for Patterned Wafers and PCB's

G. Nelissen
ELSyCa NV
Zellik, Belgium

B. Van den Bossche, M. Purcar, and J. Deconinck
Vrije Universiteit Brussel
Belgium

Abstract

Mass transfer effects and reactor design play an important role in the plating process of electronic interconnects. To improve the behaviour and performance of the plating reactors used for electronic modules, a better understanding of the electrolyte flow, current density distribution and deposit thickness distribution in the plating reactor is needed. In this paper a simulation tool will be presented that allows calculating the current density and deposit distribution in arbitrary shaped three dimensional electrochemical reactors. Calculations of current density distributions on a resistive wafer and on a patterned wafer will be shown.

Introduction

Although advanced numerical methods exist and have been applied with great success in a broad range of engineering domains (hydrodynamics, aerodynamics, structural mechanics, and heat transfer), the use of these methods for electrochemical applications remains very limited. One of the main reasons for this might be the complexity of the processes that govern electrochemical reactors. The main processes are: electrochemical kinetics at electrodes, hydrodynamics of the electrolytic solution, mass transport of ions and uncharged species due to convection, diffusion and migration, and eventually also homogeneous reactions, gas evolution, heat generation in the bulk and at the electrode-electrolyte interfaces.

Ideally, a numerical software system should treat (almost) all the effects described above to simulate an electrochemical process.

In this work, simulations are performed with the ELSY3D (v0.1) software tool¹, and take into account the following phenomena:

- ohmic drop in the electrolyte solution;
- cathodic polarisation (Butler-Volmer);
- reactor configuration
- active surface fraction of the different pattern zones
- electrical contacting method and injected current.

This modelling approach is commonly denoted as the 'potential model'. In order to produce reliable simulation results, the physico-chemical input parameters (polarisation behaviour, conductivity) need to be defined carefully.

Mathematical Model

Cathodic Reaction

Although cathodic deposition reaction mechanisms can become very complex, the polarisation behaviour for single metal deposition processes $Me^{z+} + ze^- \rightarrow Me$ is often quite accurately described by a Butler-Volmer type relation²:

$$j_n = j_0 \theta \left(e^{\frac{\alpha_a F}{RT}(V-U-E_{01})} - e^{-\frac{\alpha_c F}{RT}(V-U-E_{01})} \right) \quad (1)$$

Where j_n is the amplitude of current density normal to the electrode surface, j_0 is the exchange current density, R the gas constant, T the temperature, α_a and α_c anodic and cathodic charge transfer coefficients, and E_{01} the equilibrium potential for the deposition reaction.

For an electrode surface covered with very small features (micro-size range), the effect of a surface active fraction θ being < 1 , can simply be taken into account in the Butler-Volmer expression (1), since the current density distribution on the micro-scale features is uniform.

The local variation of the metal thickness d for a certain time step Δt is simply computed from Faraday's law:

$$\Delta d = \frac{M \Delta t j_n}{\rho z F} \quad (2)$$

assuming a 100% efficiency for the deposition process. M holds for the atomic weight of the metal, ρ for the density, z is the number of electrons exchanged in the metal deposition reaction, and F is Faraday's constant.

Anodic reaction

The main reaction that occurs at inert impressed current anodes is oxygen evolution. Due to the thin passivation layer that is often present on the surface of this type of electrodes, the polarisation behaviour is approached by a linear relation:

$$j_n = A(V - U - E_{O_2}) + B \quad (3)$$

with A, B polarisation constants and E_{O_2} the equilibrium potential for the oxygen evolution reaction. Anode polarisation effects are of minor importance – at least from a modeling point of view – if the anodes are at respectable distance from the cathode surface (which is certainly the case here).

Electrolyte

It is assumed that the electrolyte is well stirred or refreshed, so that it does not suffer from any mass transport problems, and only charge transport with normal ohmic resistivity effects is to be considered. Hence the potential model holds, being described by the Laplace equation² for the electrolyte potential U :

$$\bar{\nabla}(\bar{j}) = 0 \quad \bar{j} = -\sigma \bar{\nabla}U \quad (4)$$

On insulating boundaries, the current density perpendicular to the surface should be zero, which results in the following boundary condition:

$$\bar{j} \cdot \bar{1}_n = j_n = -\sigma \bar{\nabla}U \cdot \bar{1}_n = \sigma Q = 0. \quad (5)$$

On electrodes, j_n is given by equations of type (1) or (3).

Numerical Solution Method

BEM Approach for Electrolyte and Electrode Reactions

As the conductivity of the electrolyte is constant, the Boundary Element Method³ (BEM) is to be preferred over other (volume) discretisation methods as for example the Finite Element Method⁴ (FEM) or the Finite Difference Method (FDM), to solve the simplified charge conservation equation (4). When the BEM is applied, only the boundaries of the domain must be discretised. Another advantage, in particular for electrochemical systems, is that the current density distribution along the electrodes is a direct unknown to the problem, rather than a variable that has to be computed afterwards from the derivative of the potential field perpendicularly to the electrodes. This implicates that BEM is the more accurate method for potential problems, compared to FEM or FDM.

The characteristic BEM equation for the contribution to a point i is³:

$$c^i U^i + \int_{\Gamma} U \frac{\partial w^*}{\partial n} d\Gamma = \int_{\Gamma} w^* Q d\Gamma \quad (6)$$

with $w^* = 1 / 4\pi r$ the 3D Green function (r being the position relative to point i) and $Q = \partial U / \partial n$ the inward flux on the boundary nodes. c^i is an integration constant for point i . Γ is the 2D surface that encloses the 3D computational domain. In order to apply BEM, the boundary Γ is to be discretised into a series of N non-overlapping elements, transforming equation (6) into:

$$c^i U^i + \sum_{k=1}^N \int_{\Gamma_k} U \frac{\partial w^*}{\partial n} d\Gamma = \sum_{k=1}^N \int_{\Gamma_k} w^* Q d\Gamma \quad (7)$$

The index k ranges over all elements of the domain and integration is performed over the surface Γ_k of each element. For the 3D BEM computations in this paper, triangular elements with linear shape functions for the unknown potential U and flux field Q are used, restricting the unknowns to the nodal values.

Taking into account equation (7), the BEM equations are expressed in matrix form:

$$[H] \cdot \{U\} = [G] \cdot \{Q\} \quad (8)$$

with $\{U\}$ and $\{Q\}$ unknown vectors of size N. The matrices H and G in equation (8) are fully populated and depend only on the geometry of the domain.

$$\begin{bmatrix} [H] & 1/\sigma[-G] \\ [0] & [I] \end{bmatrix} \begin{Bmatrix} \{U\} \\ \{j_n\} \end{Bmatrix} + \begin{Bmatrix} \{0\} \\ \{f(V-U)\} \text{ or } \{0\} \end{Bmatrix} = \{0\} \quad (9)$$

The system equation matrix (9) is non-linear due to the presence of non-linear polarisation relations $f(V-U)$ of type (1). It is solved using a Newton-Raphson iterative method, combined with a band Gauss algorithm to solve the linear system of equations that appears after each iteration of the Newton-Raphson procedure.

Triangular Surface Mesh Generation

The grid quality is of utmost importance for the accuracy of the results. A hybrid grid generator⁵ is used to produce the surface mesh that is required for the BEM/FEM computations. This flexible grid generator creates an unstructured or structured mesh for each surface separately, or an unstructured mesh with structured boundary zones. The mesh must be optimally refined towards zones where edge effects are expected. On the other hand, coarse elements should be generated at any other position, allowing to produce reliable numerical results with a restricted total number of elements, hence minimising the computational efforts required to solve the system of equations (9).

Cu-plating on a Resistive Wafer

First of all, it needs to be noted that the simulation of PCB's and wafers is very similar. Therefore, although in this work only results for wafers are shown, the similar simulations with similar results can be performed on PCB plating reactors. Current density distributions in printed circuit board (PCB) plating reactors and the related deposit thickness variations are extremely important for the acceptability of the plated PCB products. Too high current densities may cause short circuits between neighbouring conducting tracks, and even more important, through-holes may become too narrow for chip implantation. Therefore an accurate prediction of the deposit thickness distribution is a valuable tool in the design process of PCB's.

The distribution of the current density (or related deposit thickness distribution) can be studied on three different scales:

- level 1 : the entire reactor (macroscale),
- level 2 : particular PCB or wafer (depending on the print lay-out, mesoscale),
- level 3: through-hole or some neighbouring tracks (microscale).

At each of those levels, uniformity demands must be fulfilled. Of course, different approaches need to be used to be able to calculate the current density distributions at each different level.

In order to perform simulations at level 1, the electro-active surface distribution over the PCB's or wafers is averaged (which will severely reduce the computational efforts). This is simply accomplished by a reduction of the exchange current density j_o with θ in equation (1).

Geometry of the Reactor

The geometry of the wafer plating reactor is shown in Figure 1. For resistive wafers, two different contact situations are considered as presented in Figure 2.

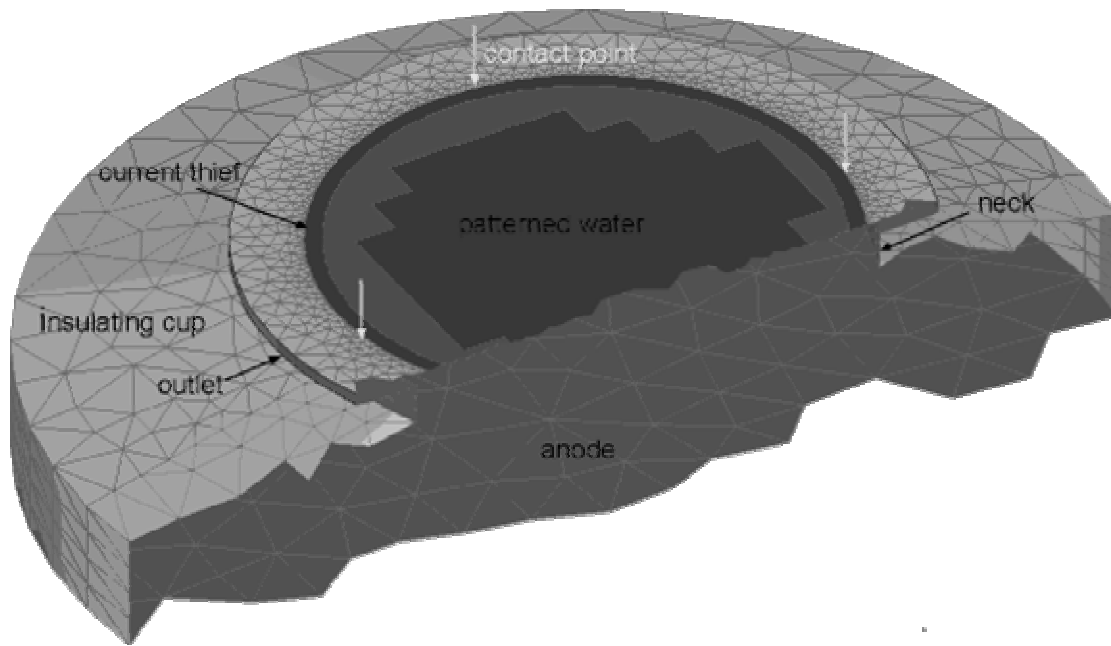


Figure 1 – Geometry and Mesh for the Cupplater

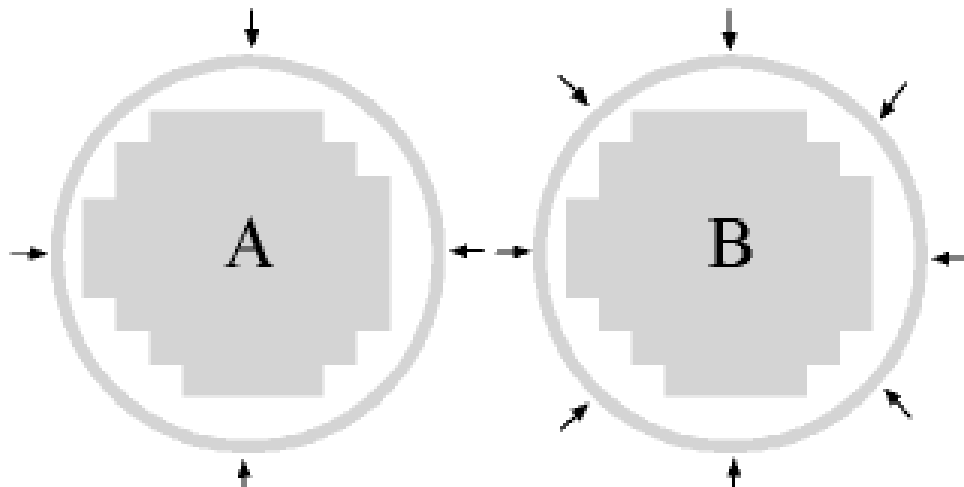


Figure 2 – Two different Contact Arrangements

Results for a Non-resistive Wafer

First, a simulation is performed for a non-resistive wafer, as a bench mark for the simulations with transient terminal effects. As the wafer is supposed to be non-resistive, the contact configuration is of no importance. The result for the deposition current density distribution is plotted in Figure 3. The current density distribution over the wafer pattern ranges from about -66.9 A m^{-2} in the middle of the wafer towards -139.1 A m^{-2} at the outer corners of the pattern. Obviously, the current thief takes away another part of the edge effects, with current densities ranging from -140.3 A m^{-2} up to -171.0 A m^{-2} . This means the current thief only takes away part of the edge effects of the active wafer patterns. The total current received by the wafer pattern is about -0.3 A (corresponding to a mean current density of -83.1 A m^{-2}), while the remaining -0.15 A passes through the current thief (mean current density = -155.4 A m^{-2}).

The total number of nodes for the triangular mesh of Figures 4a and 4b is 3520 (total number of elements = 5520), yielding a CPU time of 3660 s for 6 iterations in the Newton-Raphson procedure (hence about 10 minutes for each iteration).

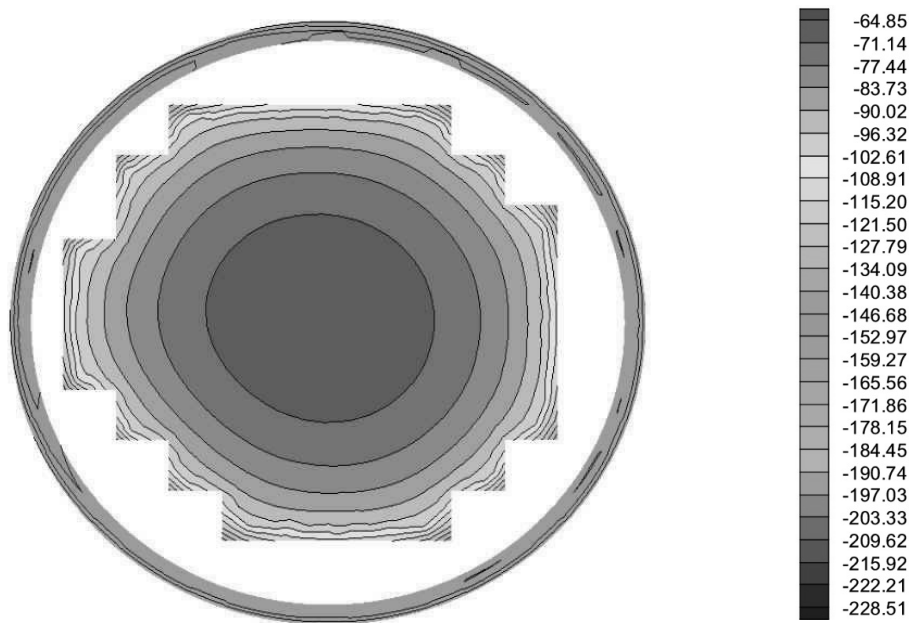


Figure 3 – Current Density Distribution (Am^{-2}) for Non-resistive Wafer

Results for a Wafer with Transient Terminal Effects

The transient thermal effect is modeled for two different contact configurations as illustrated in Figure 2.

The time steps Δt are defined with an expansion factor of 1.5, starting from $\Delta t = 1$ s. This yields a total plating time of 582 s for 14 time steps. The copper seed layer on the wafer has a thickness d of $0.1 \mu\text{m}$. After each time step, the current density distribution over the wafer pattern is compared to the result for a non-resistive wafer, and Faraday's law (2) is applied to compute the local deposit growth on the active wafer pattern and the current thief. A criterion for the end stage of the transient terminal behavior is to be defined. It is assumed that the terminal behavior becomes negligible for the time step that yields a current density distribution deflecting from the non-resistive result by at most 1 %, based on a surface integrated RMS comparison as given by equation (10).

$$RMS = \sqrt{\frac{1}{S} \int_S ((j_1 - j_2) / j_1)^2 dS} \quad (10)$$

Where j_1 and j_2 represent respectively the local current density on the active zones of the patterned wafer for the non-resistive and resistive case. Once this stage is reached for the transient simulations, the exact time point is defined by linear interpolation between the results of the last two subsequent time steps.

The current density distribution for each contacting case is plotted in Figures 4 and 5, at different time stages in the deposition process (for $t = 0$ s, 20.78 s, and 70.90 s, from left to right). The current peaks at the contact positions have nearly completely vanished after a plating time of 70.90 s. The internal initial resistivity accounts for a metal potential difference (from contacts to wafer center) of about 29 mV for arrangement A, and 17 mV for B. The metal potential difference between current thief and active wafer pattern will never completely disappear, since the connecting zone that is covered with photoresist remains highly resistive.

Both Figures 4 and 5 illustrate the advantage of an enhanced number of contact points or a contact ring to reduce – at least partly – the terminal effect. But for this example, with a rather wide current thief being present, Figures 4 and 5 also show that the peak current densities, corresponding to contact points, are mainly restricted to the current thief surface.

While the triangular mesh remains the same as plotted in Figures 4a and 4b, the CPU time of 17600 s for 6 iterations in the Newton-Raphson procedure (hence about 45 minutes for each iteration). The severely enhanced CPU times (factor 4.5 compared to the non-resistive case) are entirely due to the presence of the resistive matrix part in (12). Taking into account that about 10 time steps are required to compute the transient terminal effect, the total CPU times arrive at the limits of acceptability.

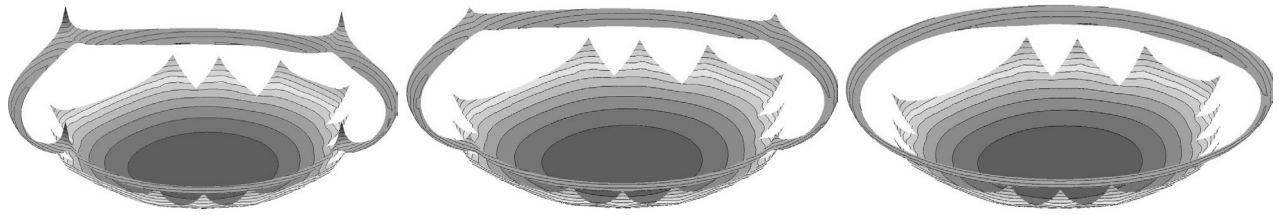


Figure 4 – Current Density Distribution for Arrangement A

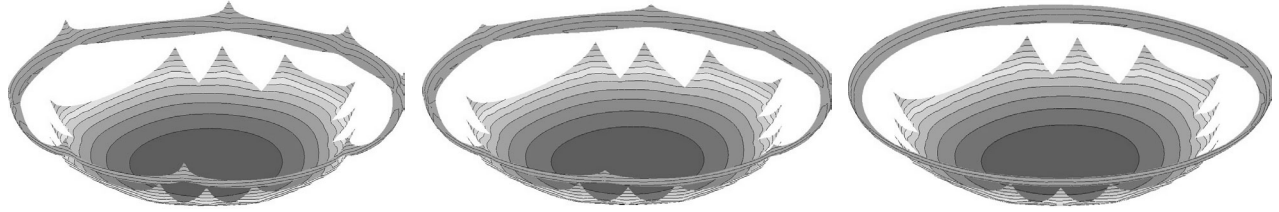


Figure 5 – Current Density Distribution for Arrangement B

Copper Plating on a Patterned Wafer

Three electrical contact clips are mounted on the holder, ensuring connection of the wafer with the current source, and meanwhile contacting the wafer with the current thief. The mean current density on the wafer surface (active pattern fraction + contact zones) is 400 A/m^2 .

The 4 inch wafer carries 4 active zones with different pattern structure, as illustrated in Figure 6. The remaining parts of the wafer are covered with photoresist.

The simulated results for the current density distribution over the wafer and current thief is plotted in Figure 7 and 8, and show a severely non-uniform behavior, not only from one pattern zone to another (due to the different surface active fraction), but also within each zone. This indicates a limited impact of the current thief, although it retrieves the major part of the current (1.06 A compared to 0.77 A for the wafer).

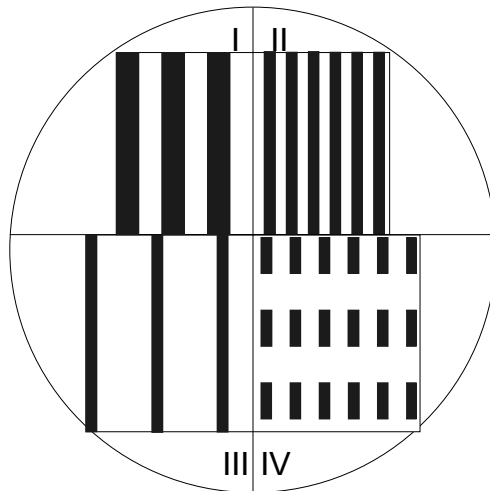


Figure 6 – Patterns on the Wafer

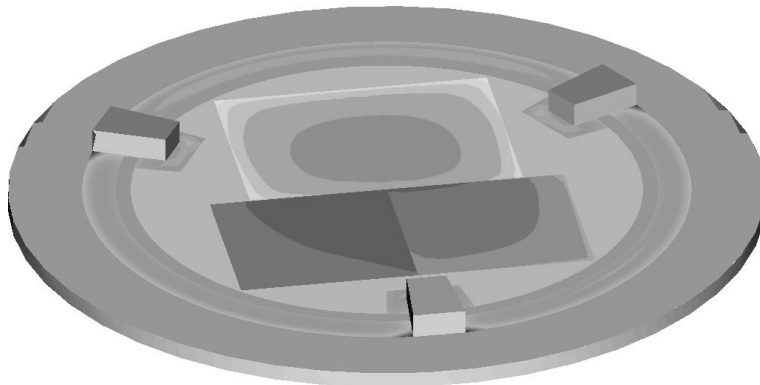


Figure 7 - Current Density Distribution over the Patterns, Current Thief and Three Contact Points

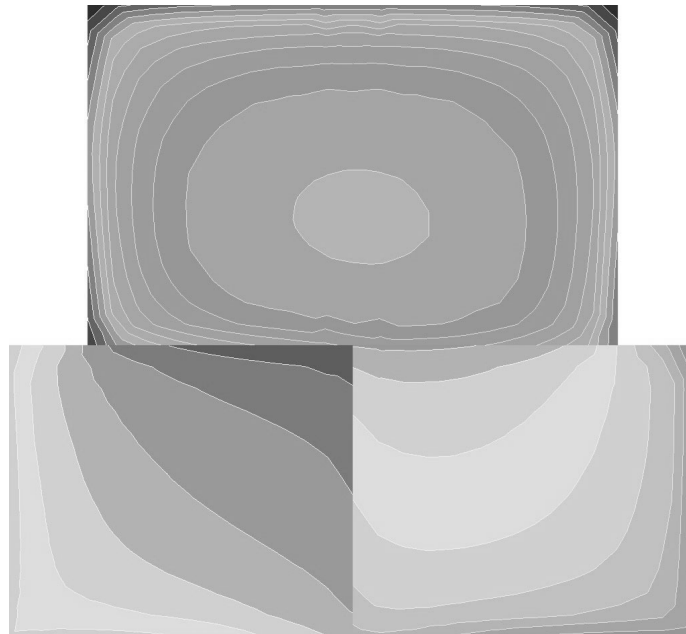


Figure 8 - Macro-scale Current Density Distribution over Zones I, II, III and IV

Conclusion

It has been shown that numerical simulation can significantly increase the understanding of the working of PCB and wafer plating reactors. The simulations include the effects of the reactor configuration, the electrode polarization the contacting method and injected currents. Both resistive and non-resistive wafers or PCB are treated.

Due to the fact that the micro-scale current density distributions over the patterns are nearly entirely uniform, abstraction can be made from the pattern geometry of each zone, and macro-scale simulations can be simply based on ‘homogenised’ wafer surfaces, with the active surface fraction of each zone incorporated in the kinetic overpotential-current density relations (e.g. Butler-Volmer). The macro-scale current density distribution on the patterned wafer zones shows a severely non-uniform behaviour, despite the presence of a current thief.

Furthermore a quantitative study and optimisation is possible using the results of the calculations. It is believed that simulations tools will become an indispensable tool to achieve breakthroughs in electrochemical engineering, especially for high-end PCB and wafer plating applications.

Bibliography

1. M. Purcar, B. Van den Bossche, L. Bortels, J. Deconinck, P. Wesselius, *Corrosion* 59 (2003) December issue.
2. J. S. Newman, *Electrochemical Systems*, Second Edition, Prentice-Hall, Englewood Cliffs, New Jersey (1991).
3. Brebbia, C.A., all, ‘Boundary Element Techniques – Theory and Applications in Engineering’, Springer-Verlag, Berlin (1983).
4. Fagan M.J., “Finite Element Analysis”, Longman Scientific and Technical, ISBN 0-582-02247-9 (1992).
5. A. N. Athanasiadis, H. Deconinck, *Int. J. Num. Methods Eng.* **58**, 301 (2003).



Three-dimensional simulations of current density distributions for patterned wafers and PCB's

Gert Nelissen, PhD.

IPC 2004, Anaheim, CA
February 25, 2004



OVERVIEW

- ELSYCA:
 - Introduction
 - Value proposition and approach
- Application: Wafer plating
- Application: PCB plating
- Conclusions



ELSYCA CORPORATION

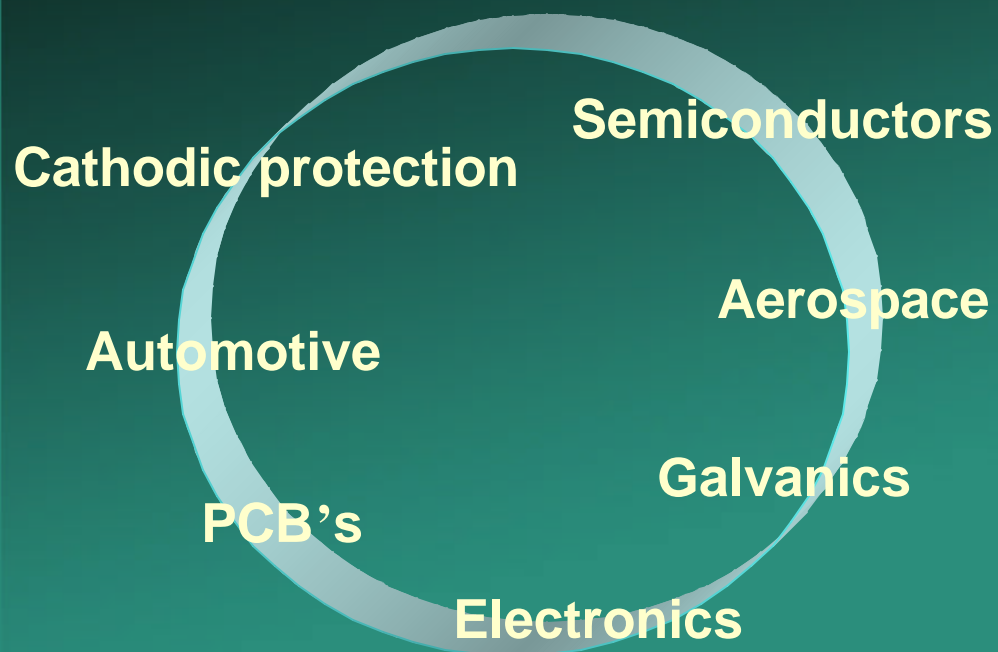
MISSION STATEMENT: To be the industry leader in electrochemical process modeling by providing state-of-the-art simulation software and expert solutions

ELSYCA provides solutions that

- speed up product development
- optimize process engineering
 - quality
 - design



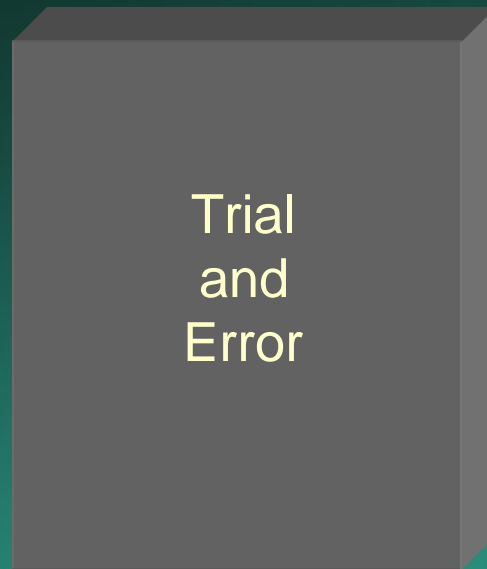
COVERING A COMPLETE RANGE OF INDUSTRIES





VALUE PROPOSITION

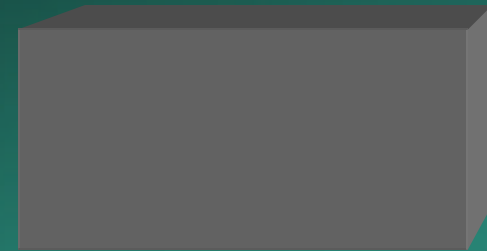
Without simulations



Trial
and
Error

- More non-uniform metal layers
- Higher process times
- Specs not attained

With simulations



- Dramatic reduction in 'trial and error' tests
- More insight in the plating process
- Improved product quality (spec's)
- Higher process speed



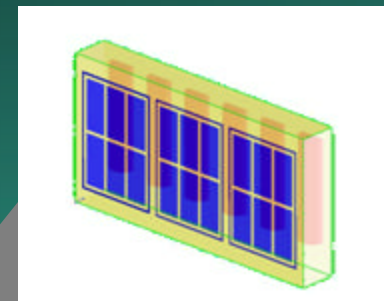
ELSYCA APPROACH

Optimized Product Quality & Processing



Physico-chemical
data gathering

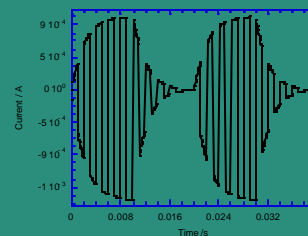
Simulation of layer
thickness distributions,
prediction of surface quality,
optimization of configuration
and process parameters



Reactor configuration
(CAD) and PCB design
(Gerber, IDF, ...)

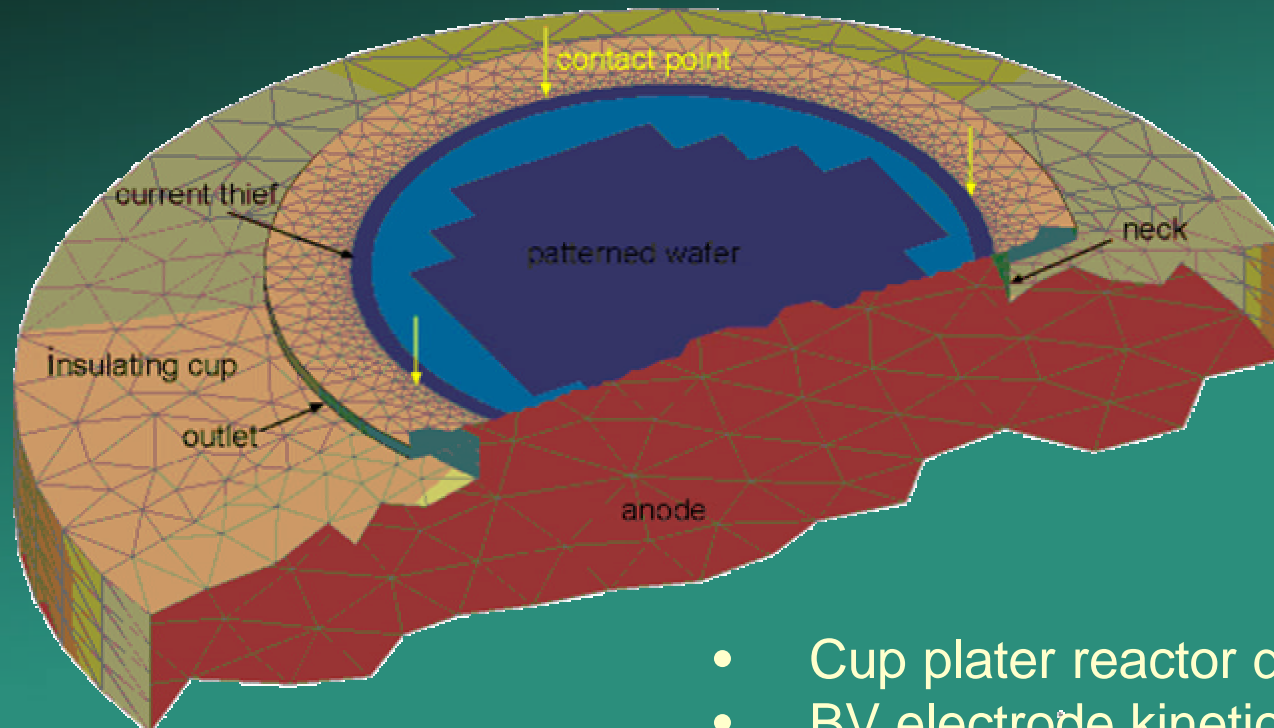


Process parameters
(current, pulse duty
cycle en frequency,
flow rate, ...)





APPLICATION: WAFER PLATING



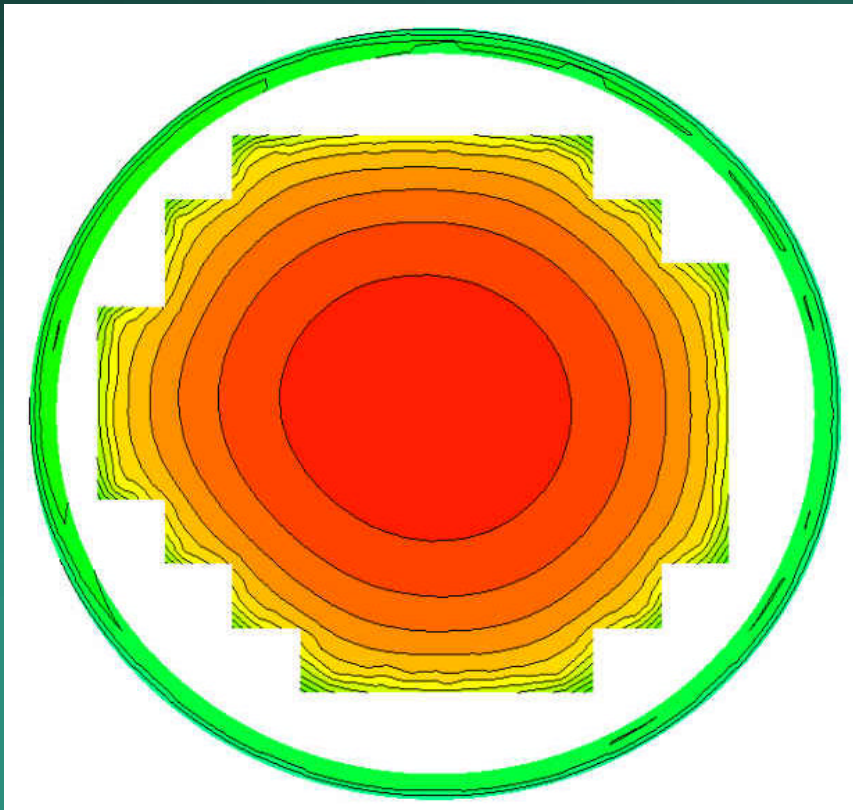
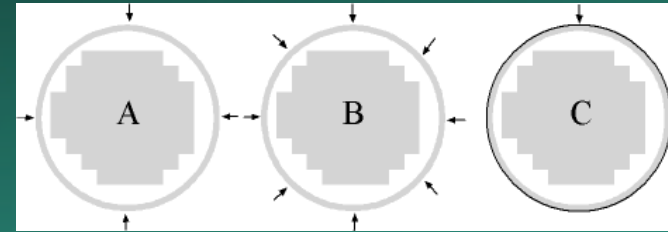
- Cup plater reactor design
- BV electrode kinetics
- DC current
- With current thief ring



ELSY3D FOR WAFER PLATING

Potential Model 3D

- Thin resistive seed layer (0.1 micron)
- Faraday's law to compute deposit growth over time steps
- Different contacting arrangements



$$\Delta d = \frac{M \Delta t j_n}{z F}$$

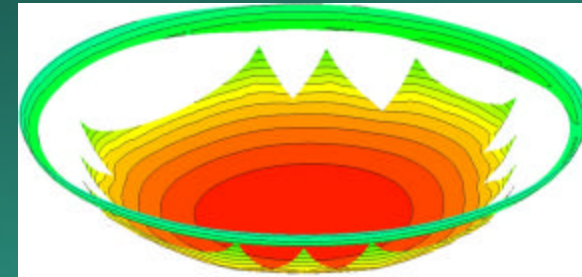
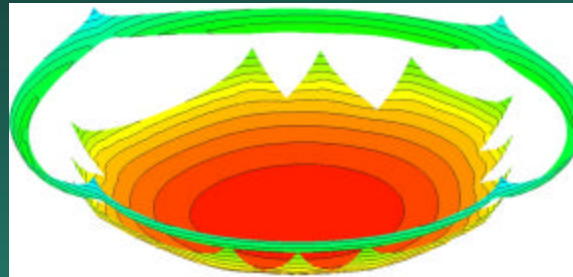
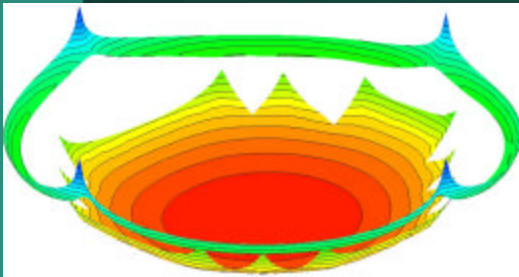
Current density
distribution for a
non-resistive
wafer



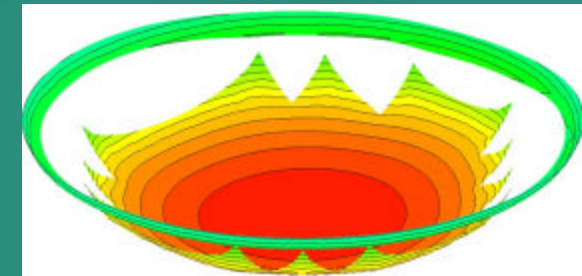
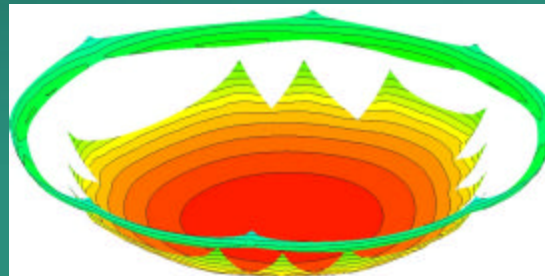
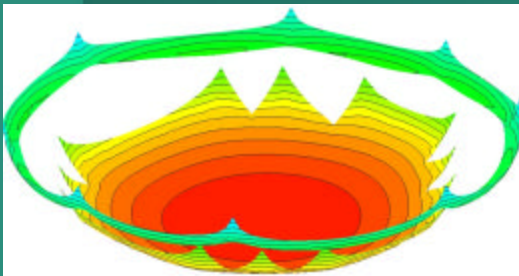
ELSY3D FOR WAFER PLATING

Current density distribution for a resistive wafer

arrangement A



arrangement B



$t = 0 \text{ s}$

$t = 20 \text{ s}$

$t = 75 \text{ s}$



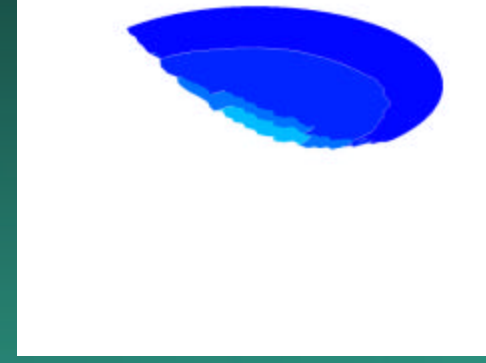
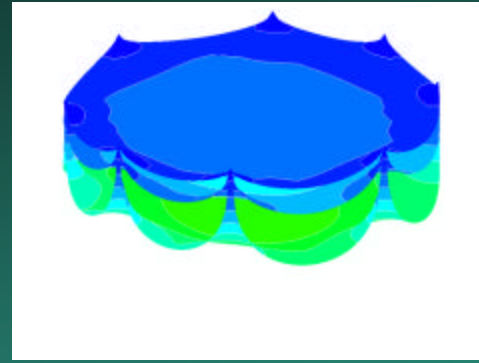
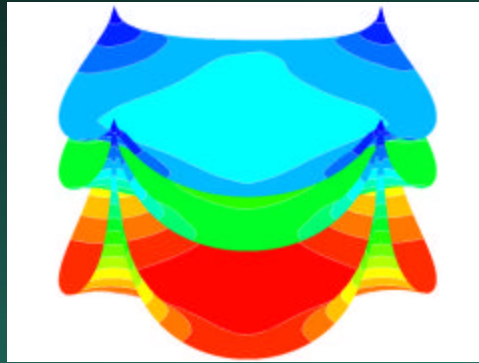
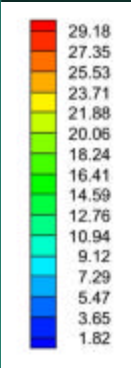
ELSY3D FOR WAFER PLATING

Electrode potential distribution

$t = 75 \text{ s}$

$t = 20 \text{ s}$

$t = 0 \text{ s}$

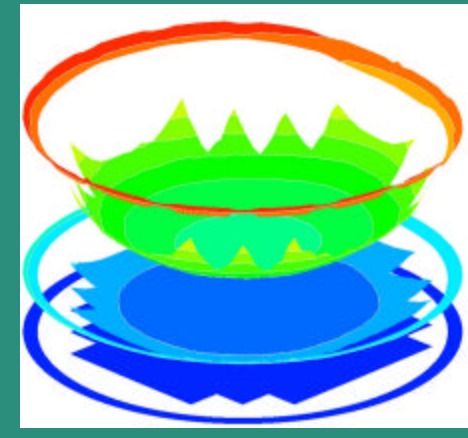
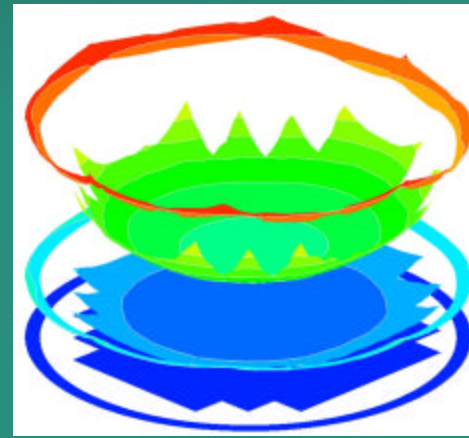
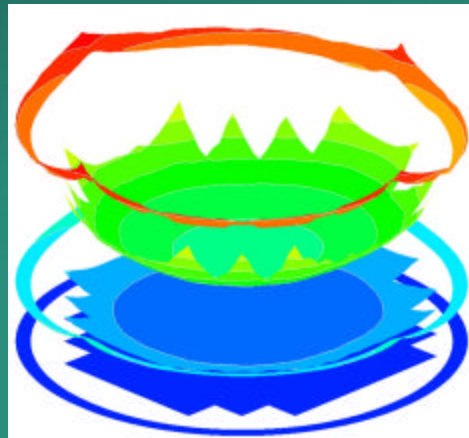
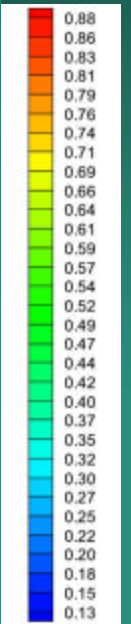


Deposit thickness distribution

$t = 75 \text{ s}$

$t = 20 \text{ s}$

$t = 0 \text{ s}$





MIOTRAS FOR WAFER PLATING

Multi-Ion Model AX

- Flow entering through holes in anode plate
- Flow leaves through narrow spacing below wafer
- Laminar fluid flow ($Re = 500$)
- Wafer placed upside down
- Axisymmetrical cross section of reactor

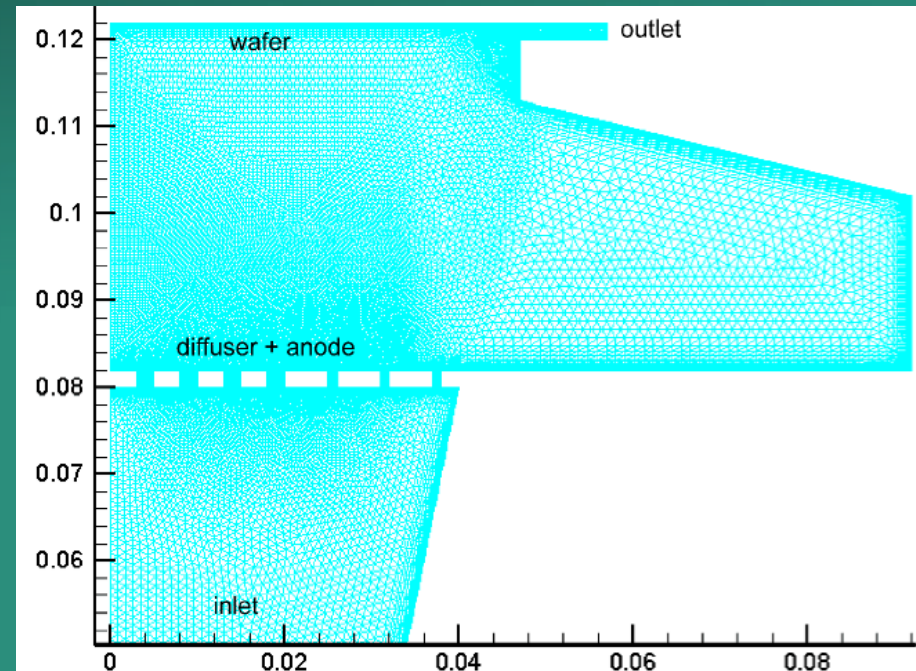
Electrode reaction



$$J = 2Fk_{od}e^{a\frac{2F}{RT}h} - k_{oc}C_{Cu^{2+}}e^{-b\frac{2F}{RT}h}$$

Copper system

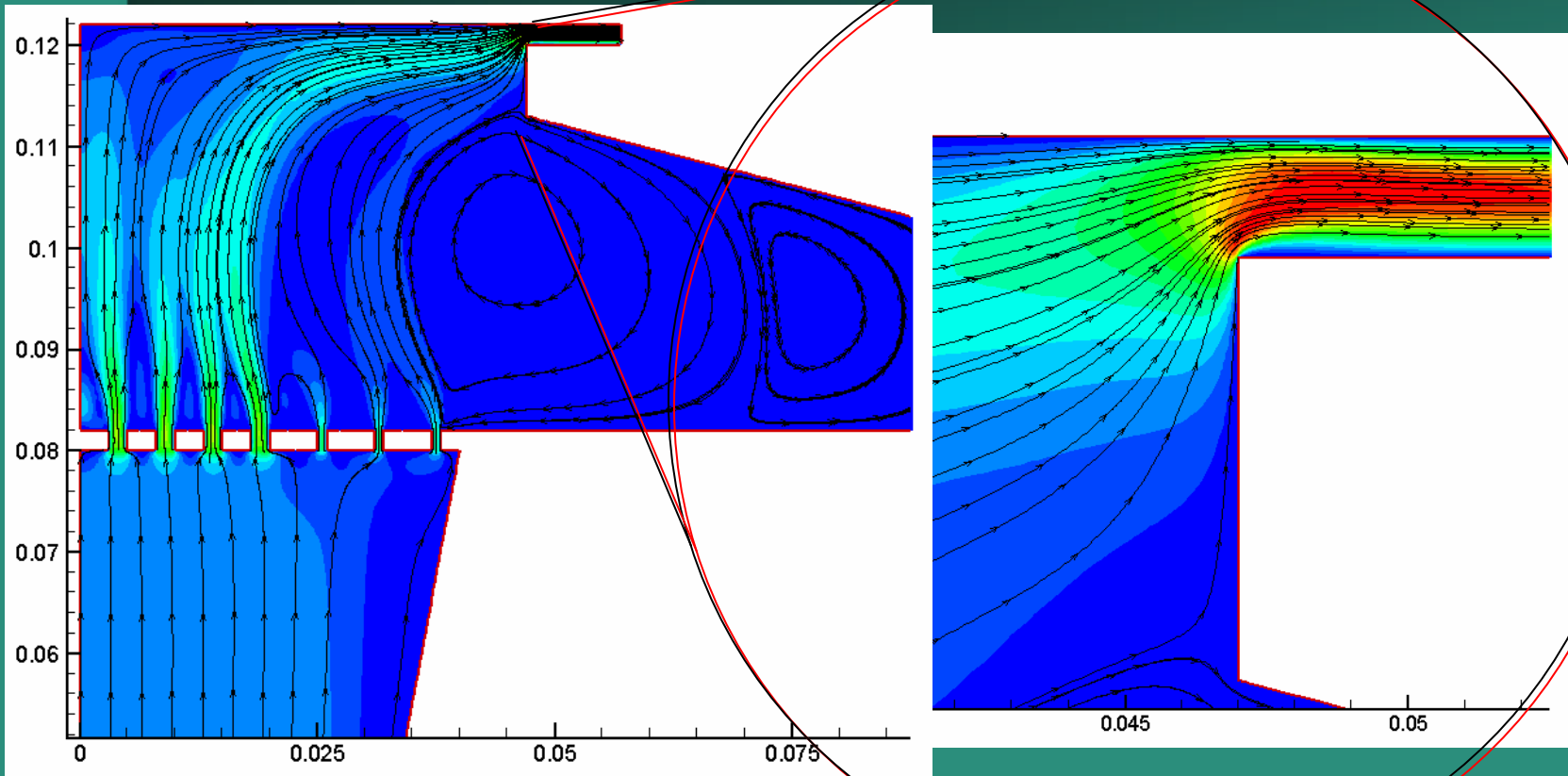
Ion	Charge z_k	Conc. / mol/m ³	D_k / m ² /s
Cu^{2+}	+2	800.0	3.5E-10
SO_4^{2-}	-2	954.3	3.9E-10
H^+	+1	714.3	3.4E-09
HSO_4^-	-1	405.7	4.9E-10





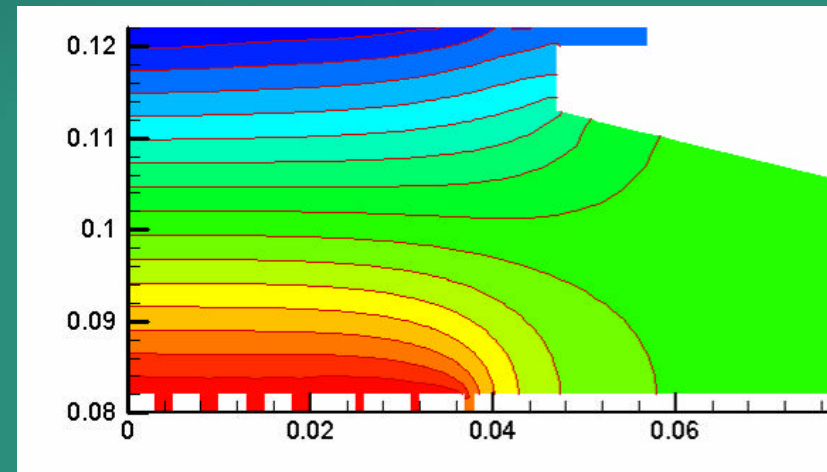
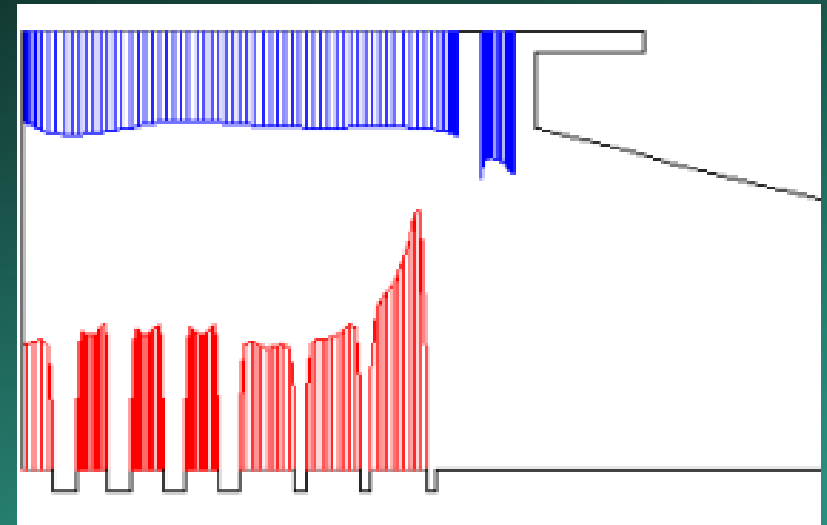
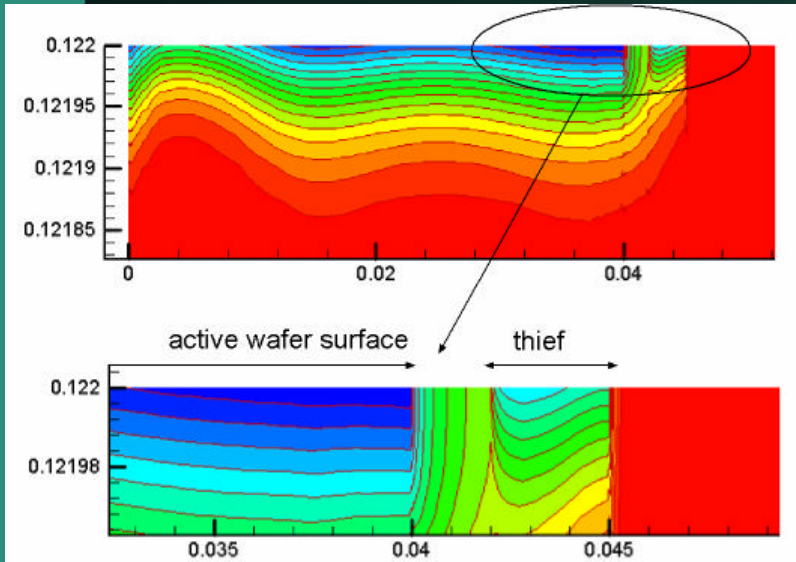
MIOTRAS FOR WAFER PLATING

Flow streamlines and intensity (color)





MIOTRAS FOR WAFER PLATING



Cu^{2+} boundary layer

Current density distribution

Electrolyte potential distribution

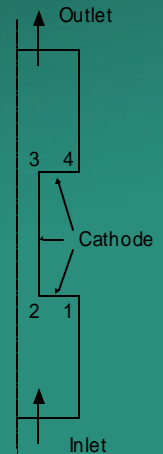
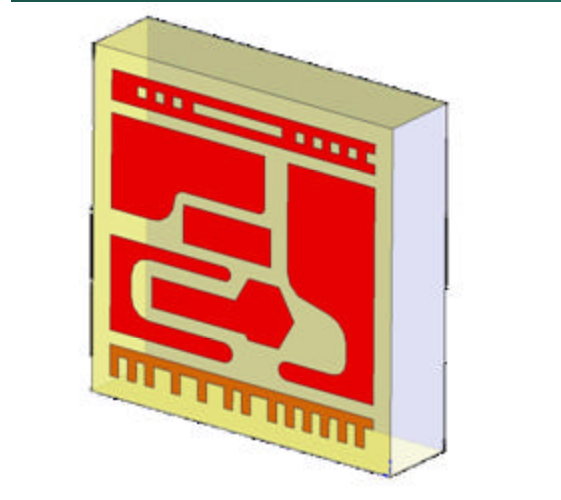
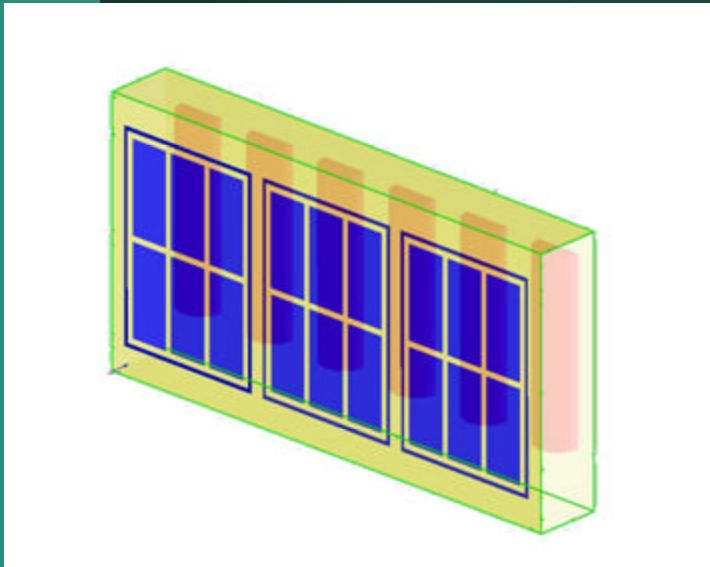


APPLICATION: PCB PLATING

Reactor scale

PCB/pattern scale

Via/TH scale



Macro scale

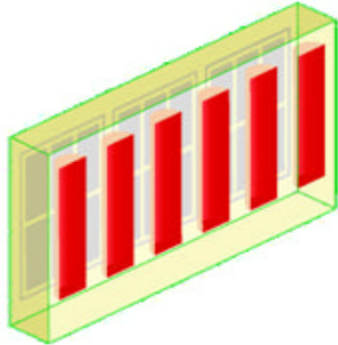
Meso scale

Micro scale



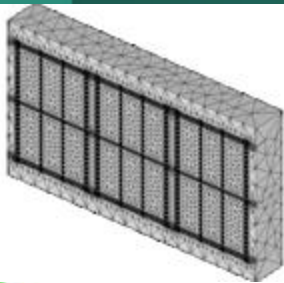
P²ST FOR PCB PLATING

Reactor scale

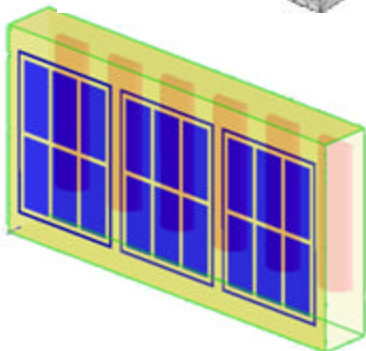


- Potential model
- BV electrode kinetics
- DC current

normal situation

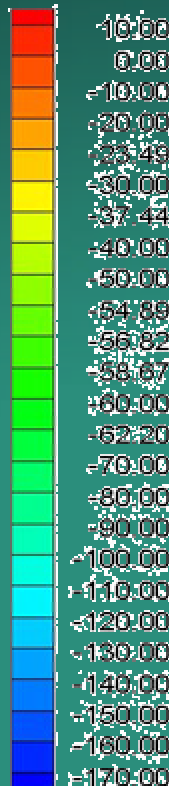
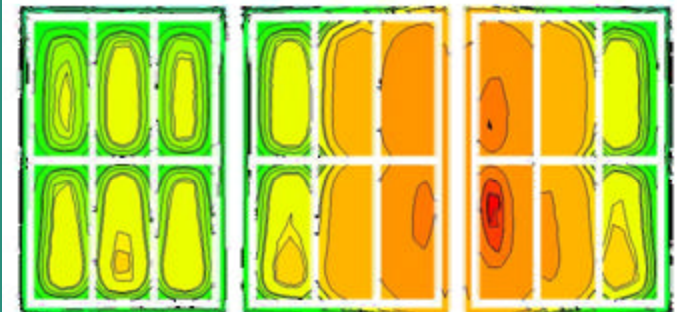
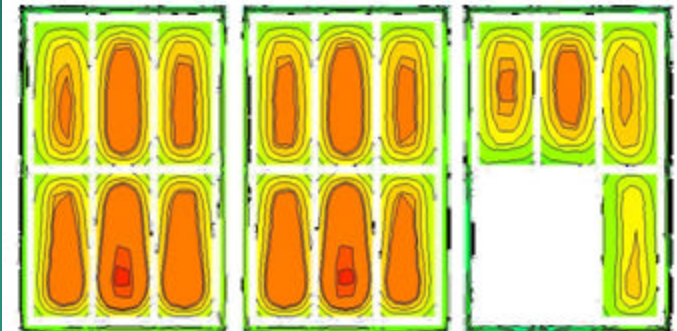
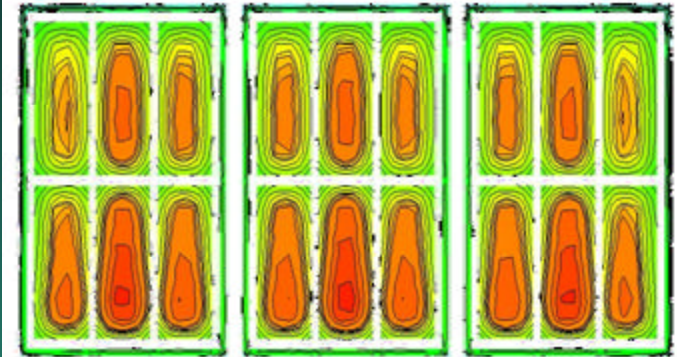


2 prints missing



2 baskets empty

Current density distribution

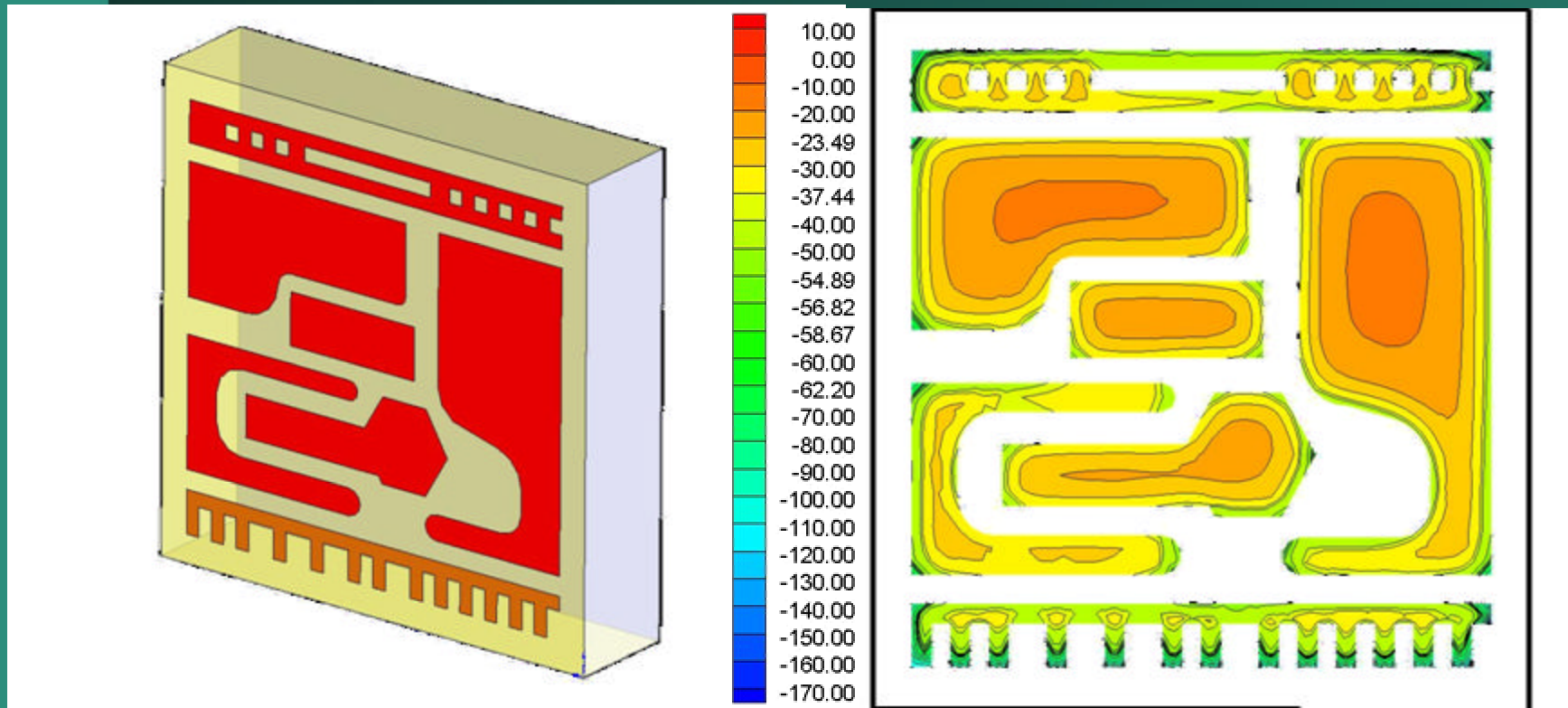




P²ST FOR PCB PLATING

PCB/pattern scale

- Potential model
- BV electrode kinetics
- DC current



PCB layout (simplified)

Current density distribution



P²ST FOR PCB PLATING

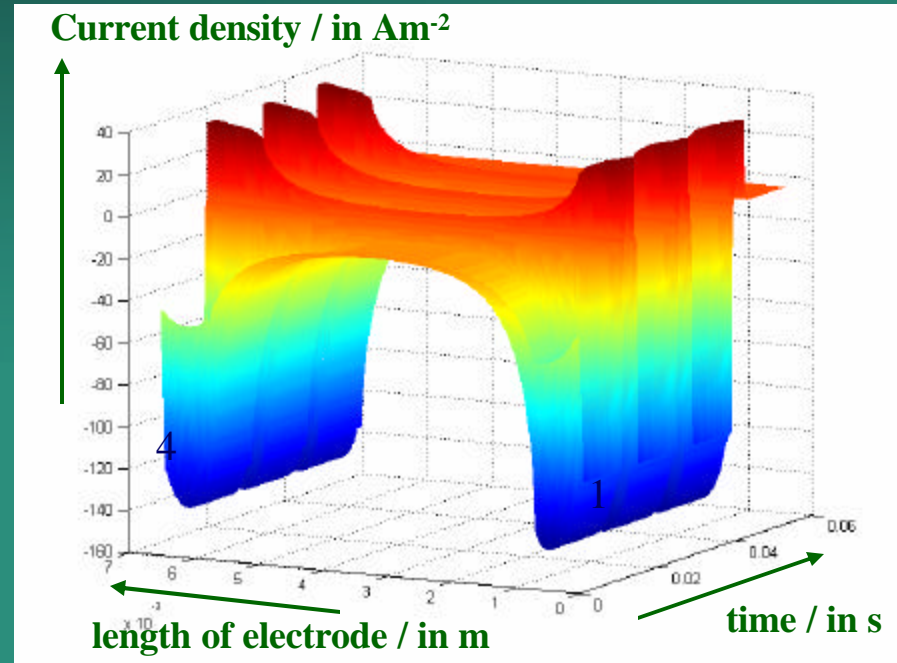
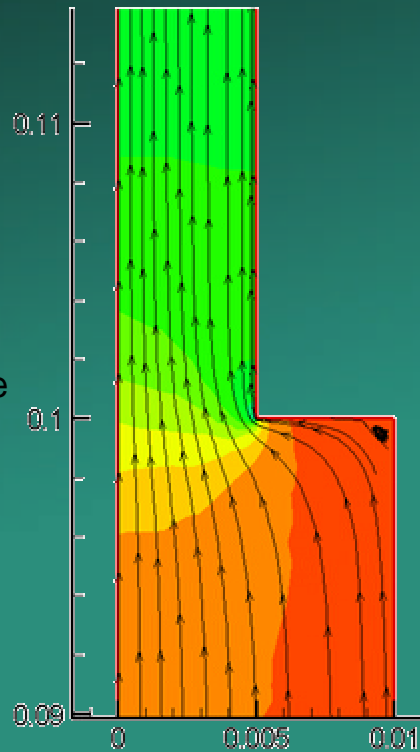
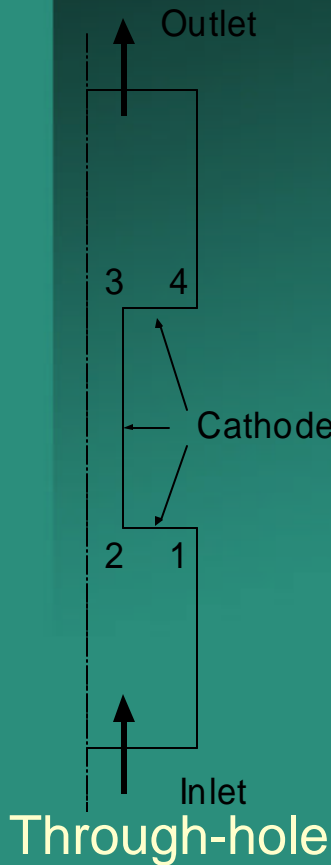
Via/TH scale

- Multi-ion model
- BV electrode kinetics
- Bipolar pulsed current

	Z	C _i (mol/m ³)	D (m ² /s)
Cu ²⁺	+2	300	5.0 E-10
HSO ₄ ⁻	-1	1800	7.0 E-10
H ⁺	+1	1200	3.5 E-9

Electrode reaction

$$J = 2Fk_{od}e^{a\frac{2F}{RT}h} - k_{oc}C_{Cu^{2+}}e^{-b\frac{2F}{RT}h}$$



Through-hole

Fluid flow

Current density distribution



P²ST: PRODUCT FEATURES

- PCB layout insertable in Gerber format, IDF, ...
- High reliability prediction of current and layer thickness distributions on macro and meso level (including PCB layout)
- High reliability prediction of current and layer thickness distributions micro level (vias, through holes)
- Automated variation and optimization of process parameters (e.g. anodic/cathodic pulse height, frequency, duty cycle, ...)
- Database available for each electrolyte bath
- Entire integration in design packages (CAD systems) or front-end systems (CAM systems)



P²ST: CUSTOMER BENEFITS

- P²ST is compatible with all front-end systems
- P²ST uses digital data sent by the customer
- P²ST predicts with a high reliability what the plating performance will be (e.g. Cu-thickness & distribution)
- By using P²ST, engineering can simulate performance by adjusting wave forms, current densities, etc.



CONCLUSIONS

ELSYCA's integrated approach and unique software solutions guarantee:

- Shorter time-to-market on new product introduction
- Quicker turn around time
- Optimised product quality, processing & design
- In-depth understanding & control of electrochemical process